Microwave-Assisted Preparation of Luminescent Materials

Subjects: Nanoscience & Nanotechnology

Contributor: Jose Miranda de Carvalho

Luminescent inorganic materials are used in several technological applications such as light-emitting displays, white LEDs for illumination, bioimaging, and photodynamic therapy. Usually, inorganic phosphors (e.g., complex oxides, silicates) need high temperatures and, in some cases, specific atmospheres to be formed or to obtain a homogeneous composition. Low ionic diffusion and high melting points of the precursors lead to long processing times in these solid-state syntheses with a cost in energy consumption when conventional heating methods are applied. Microwave-assisted synthesis relies on selective, volumetric heating attributed to the electromagnetic radiation interaction with the matter. The microwave heating allows for rapid heating rates and small temperature gradients yielding homogeneous, well-formed materials swiftly. Luminescent inorganic materials can benefit significantly from microwave-assisted synthesis for high homogeneity, diverse morphology, and rapid screening of different compositions. The rapid screening allows for fast material investigation, whereas the benefits of enhanced homogeneity include improvement in the optical properties such as quantum yields and storage capacity.

Luminescent Inorganic Materials | Microwave-Assisted Synthesis

1. Introduction

Luminescent materials, also known as phosphors, usually refers to inorganic materials that emit light after external physical stimuli, such as UV-VIS, IR-Lasers, X-rays, γ-rays, and e-beams [1]. These materials are composed of a host lattice with intentionally added optically active impurities (dopants). The dopants act as luminescent centers, converting the incident excitation into a characteristic light emission that depends on the dopant's identity [2]. The most common dopants for luminescent materials are the f-metals, such as the trivalent rare-earths (RE^{3+}: Pr, Nd, Eu, Tb, Dy, Er), that emit light after optical transitions within the f-electron manifold [2]. The f-electrons are strongly shielded from the chemical environment and retain atomic characteristics, yielding sharp emission lines with wavelengths nearly independent of the host's composition. The f-f electronic transitions are parity forbidden and, thus, the emission decay times are long (μs-ms).

Some rare earth ions (e.g., Ce^{3+}, and Eu^{2+}) behave as crystal-field sensitive ions, having intense broad emission bands with emission color dependent on the host's composition. In these cases, the emission is governed by parity-allowed 4*f*-5*d* transitions, yielding intense emission bands with fast decay times (ns-μs). Figure 1 provides the comparison between the *f-f* and *f-d* transitions for the Eu^{3+} and Eu^{2+} ions.

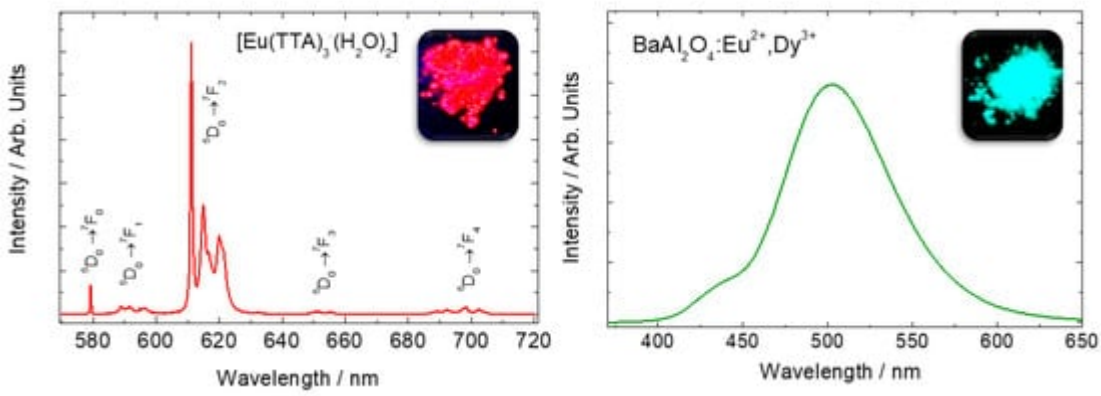

Figure 1. Emission spectra of Eu^{3+} in $Eu(TTA)_3{\cdot}(H_2O)_2$ complex (**left**), and Eu^{2+}-doped $BaAl_2O_4$ host (**right**). Eu^{3+} sharp lines spectra is attributed to f-f transitions whereas the Eu^{2+} broad emission band is attributed to f-d transitions. Adapted from references [3][4]. Copyright © 1997 Published by Elsevier B.V.

Various transition metals also act as luminescent centers, e.g., Mn^{4+}-doped K_2SiF_6 [5], and Cr^{3+}-doped $ZnGa_2O_4$ [6]. In these cases, parity-forbidden d-d electronic transition is responsible for the emission. The d-orbitals broadly interact with the chemical environment leading to strong crystal field splitting according to the composition of the materials. Thus, most of the transition metals' absorption and emission bands are broad. However, sharp emissions can also be observed, such as Mn^{4+}-doped K_3ScF_6 red phosphors [7].

Luminescent materials can act as light converters due to different photophysical processes, such as downconversion (or quantum cutting) [8][9][10], upconversion [11][12][13], and down-shifting [14][15] (Figure 2A–C). Downshifting is the most conventional photoluminescence mechanism, where high-energy photons are converted into low-energy photons. Ideally, all excited photons are converted to emitted photons without losses in the optical process, obtaining a quantum yield of 100% [16][17][18][19]. On the other hand, the first experimental evidence for quantum yields higher than 100% was reported for $YF_3:Pr^{3+}$ material [17][20]. This optical phenomenon proposed by Dexter consists of the high-energy photons splitting into two or more lower-energy photons. This mechanism, called downconversion or quantum cutting, involves single or multiple ions (e.g., in $YF_3:Pr^{3+}$ [17][20] or $YPO_4:Yb^{3+}$, Tb^{3+} [10], respectively).

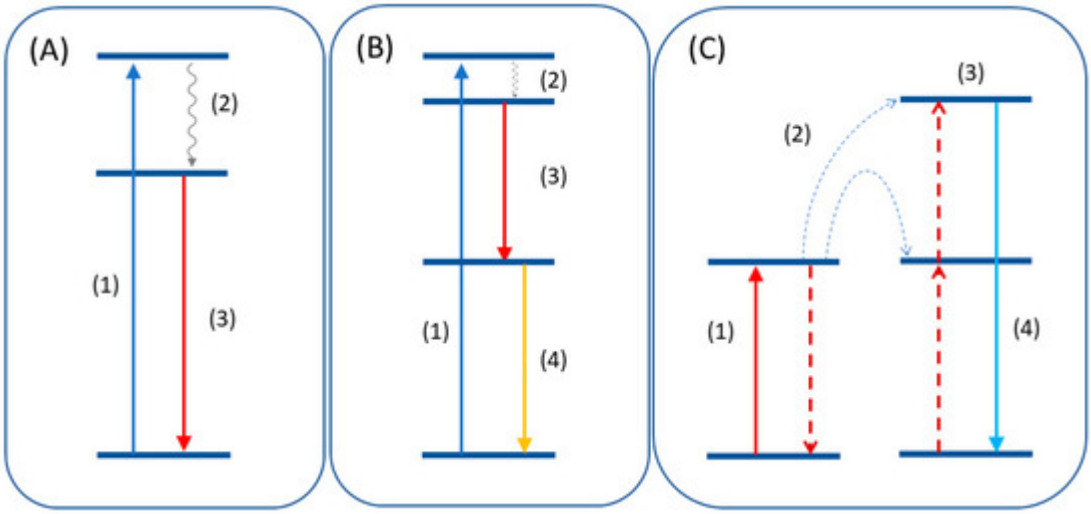

Figure 2. (**A**) Downshift mechanism consisting of excitation (1), non-radiative decay (2), and emission (3). (**B**) Quantum cutting mechanism where the emission of two photons (3,4) occurs after the excitation. (**C**) Upconversion emission after energy transfer (2) of two lower energy quanta to a higher excited state (3).

Upconversion (UC) is a nonlinear optical phenomenon that converts two or more low-energy photons to a higher-energy photon [13]. This optical process, known as anti-Stokes emission, was theoretically proposed by the physicist Nicolaas Bloembergen in 1959 [21]. The first experimental result, reported by François Auzel in 1966, consisted of the energy transfer from Yb^{3+} to Er^{3+} and Tm^{3+} ions [13]. The UC process has since inspired light conversion mainly from near-infrared (NIR) to UV-visible-NIR light, suitable for bioimaging, solar cells, anticounterfeiting, photocatalysis, and photodynamic therapy [22].

Persistent luminescence (PeL) materials continue to emit light after removing the excitation source due to stored energy in the structural defects that act as charge carrier traps [23][24][25]. After the removal of the excitation, the material absorbs available thermal (kT) or optical (hv) energy to release the trapped charge carriers that recombine with the emitting centers. The radiative decay of the excited states emits a photon with a characteristic wavelength. The most efficient PeL phosphors are dominated by Eu^{2+}-doped inorganic materials, exhibiting 24 to 48 h of persistent emission after few minutes of excitation in the UV-VIS range [25]. However, plenty of examples for d- and f-metals are available, and extensive reviews on the topic have been published [23][24].

Luminescent materials have several applications in technology, telecommunications, and health sciences, and are the subject of extensive research. Specific applications can be in light-emitting diodes [26][27][28], laser [29], thermometry [30], thermoluminescence dating [31][32], dosimetry [33], bioimaging [6][34], and photodynamic therapy [35][36][37].

For instance, phosphor converters for LEDs (pc-LEDs) work as light converters where an excitation source, e.g., blue emitting-LEDs, excites the luminescent material that emits broadband in the yellow region. This kind of phosphor has defined characteristics, such as high quantum yields and fast excited-state decay times. The most efficient light converters for pc-LED are inorganic hosts doped mainly with Ce^{3+} and Eu^{2+} [27][38][39][40]. The parity-allowed (f–d) electronic transition in Ce^{3+} and Eu^{2+} ions results in high-intensity emissions with short excited-state lifetimes (µs-ns). However, other examples can be easily found in trivalent rare earths, Eu^{3+}, Tb^{3+}, Pr^{3+}, Dy^{3+}, and *d*-metals (Mn^{4+}) doped materials [5][7][41][42][43][44]. PeL materials are in evidence nowadays due to vast and unexplored bioimaging applications [37], theranostics [45], and photocatalysis [46]. When it comes to application, persistent phosphors must have high quantum yield and high storage capacity [47][48].

2. Concepts and Mechanisms of Microwave Heating

Microwaves (MW) are electromagnetic radiation in the frequency interval of 300 MHz (1.24 µeV; 1 m) to 300 GHz (1.24 meV; 1 mm). Radiation in this range is mainly used in wireless telecommunication protocols, such as Bluetooth and wi-fi modems [49]. A narrow part of the microwave spectrum is used for industrial, domestic, scientific, and medical purposes (ISM bands) [50]. The industrial and domestic uses of microwaves come from the

ability to heat certain materials depending on their dielectric properties [49][51]. For instance, the radiation in a domestic microwave oven (2.45 GHz; λ: 12.2 cm) interacts with the water contained in the food, heating it swiftly due to the intrinsic dielectric properties of the water molecules. Further, a precise tuning of microwave radiation parameters enables microwave heating of different materials, such as metal oxides [52][53], carbon [49][54][55], and organic solvents [56].

Microwave heating properties differ significantly from conventional heating ones. In conventional heating, the external source, such as a resistive furnace, heats the material's surface, leading to a large temperature gradient compared to the material's core. Instead, dielectric heating occurs volumetrically, meaning that the material irradiated by the microwaves is heated locally, leading to a small temperature gradient [56] (Figure 3). Microwave-assisted heating rates are drastically steeper than conventional heating because of the absence of heat transfer from an external source.

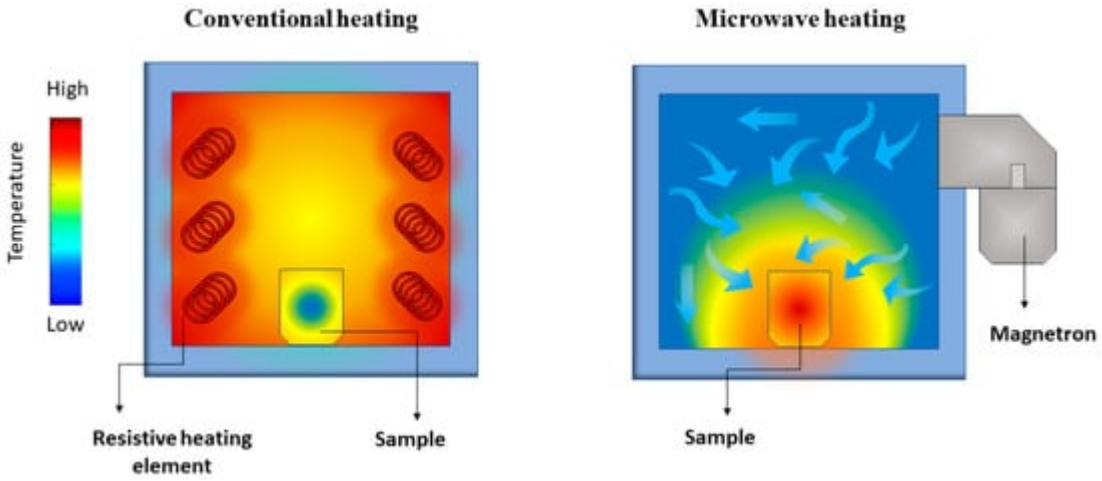

Figure 3. Representation of the temperature gradient in conventional (**left**) and microwave-assisted (**right**) heating of a solid sample.

The combination of these properties can be highly beneficial to the synthesis of inorganic materials using microwave-assisted approaches. For instance, solid-state methods benefit significantly from dielectric heating, shortening the synthesis time from days and hours to tens of minutes. In addition, it can yield more uniform, homogeneous materials [57].

The principles of microwave heating are based on the material's response to the electromagnetic fields' alternating nature. Bhattacharya et al. [49] discussed in detail the microwave heating mechanism in several materials. The relevant parameters for the heating include the dielectric constant (ε′) and dielectric loss (ε″). The parameters can be interpreted as the ability of the material to store (ε′) and convert (ε″) the electric energy from the microwave irradiation.

The main mechanism of dielectric heating is attributed to the polarization losses that comprise dipolar, interfacial, ionic, and electronic losses [49][51]. All these contributions are related to the intrinsic properties of the materials.

Thus, a corrected assessment of the microwave interaction with a particular material must include a detailed analysis of its dielectric properties. Additionally, if the material to be irradiated has high conductivity, then the conduction loss enters the summation in the dielectric loss constant (ε″). Magnetic contributions must be considered when the material presents a magnetic moment. Most luminescent materials are not intrinsically magnetic, making it possible to simplify the equation to only the electric contribution.

The interaction of microwaves with matter can be understood as how much a microwave can penetrate in a specific material. The penetration depth of a microwave within materials interacting only with the electric field (μ''_r = 0) can be expressed by Equation (1):

$$dp = \frac{c}{\sqrt{2\pi f}\sqrt{\varepsilon'_r \mu'_r}}\left[\left(\sqrt{1+\tan^2\delta_\varepsilon}\right)-1\right]^{-1/2} \quad (1)$$

where *f* is the frequency of the microwave, (ε'_r) is the relative dielectric constant, and (ε''_r) is the relative dielectric loss. The loss tangent (is an important parameter that denotes the dissipation of the electrical energy quantitatively due to multiple physical processes [58], and can be defined by Equation (2):

$$\tan\delta_\varepsilon = \frac{\varepsilon''_r}{\varepsilon'_r} \quad (2)$$

The *dp* parameter will then classify the materials' interaction with the microwave in three different classes, (i) opaque or reflector, (ii) transparent, and (iii) absorber [49]. If the penetration depth is shallow (micrometer range), the microwave is reflected by the material's surface. Typical examples of microwave reflectors are metals like Cu (*dp* = 1.3 μm) and Al (*dp* = 1.7 μm). Alternatively, if the penetration depth is too large, then the microwave goes through the material without any interaction being transmitted. Materials like alumina, borosilicate glasses, and zirconia are excellent examples of microwave-transparent materials, with penetration depths larger than 10 m.

Neither of these situations is ideal for heating the materials and therefore performing microwave-assisted synthesis. To interact with microwaves, the radiation's penetration depth must be optimal to dissipate the electrical energy efficiently. Absorber materials have penetration depths in the order of centimeters, such as SiC (*dp* = 1.9 cm), water (3.0 cm), and carbon black (5.7 cm) [59][60][61]. The tangent loss of the materials in terms of reflector, transparent and absorber have typical values of

< 0.01 (transparent), >0.1 (absorbers), and >>1 (reflectors).

The fact that the dielectric properties of the materials can vary with temperature increases possibilities of interacting with materials by changing their reactional medium temperature. For instance, yttria-stabilized zirconia is microwave-transparent up to 200 °C (

;), suffering a transition to an absorber material at 600 °C (;

). The principle of intrinsic tangent loss modulated by the materials' temperature is beneficial for synthetic purposes. A synthetic precursor consisting of a mixture of low-lossy materials (transparent) can be in close contact with a high-lossy (absorber) material that will initially interact with the microwave, generating local heating. The heat transfer to the low-lossy material can inflict a change in the tangent loss, transitioning from transparent to absorber. This type of heating can be denominated as hybrid microwave heating, and it is the most-used method in microwave-assisted solid-state (MASS) synthesis [49][51][62][63].

3. Properties of Microwave Heating

Microwave-assisted heating can be characterized by a combination of unique properties offering faster and more efficient heating, often leading to more crystalline, homogeneous materials [64]. Firstly, the direct energy conversion into heat leads to a smaller temperature gradient throughout the precursors. In conventional resistive heating, the large temperature gradients make the reactions sluggish, taking a long time to reach equilibrium and generate the products. Dielectric heating works in the opposite manner, heating the materials from the inside to the outside. Dielectric heating leads to minimal energy consumption and faster reaction rates [65]. The thermal efficiency is an appealing point when considering laboratory work for sample screening and compositional tailoring. High throughput can be obtained with specialized setups, allowing the synthesis of tens of samples in few minutes. The fast screening in compositional tailoring can be beneficial for luminescent materials with a strong correlation of the optical property with the composition and structure.

Dielectric heating is also volumetric by nature, meaning that the heating is uniform throughout the sample, in theory. In actual samples, the volumetric heating is not perfect due to inhomogeneity in the precursors and temperature dependence of the dielectric properties [66]. However, compared with conventional heating, the MASS method has more uniform heating and, therefore, a more homogeneous composition of the final products. For luminescent materials, this property is of utmost importance once the homogeneous dispersion of activator and sensitizer ions in the material's host leads to higher quantum yields and increased brightness [67]. Homogeneous luminescent materials offer a more defined local structure that can lead to precise control of the emitting color of crystal field-sensitive ions, such as Eu^{2+} [57].

The ionic diffusion limit encountered in conventional heating methods is also a significant problem in solid-state synthesis [64][68]. Usually, the diffusion is exceptionally slow if the temperature of the synthesis is lower than two-thirds of the precursor's melting point (Tamann's rule) [69], which translates to temperatures usually higher than 1000 °C. The microwave radiation effect on ionic diffusion in bulk inorganic materials was investigated by Whittaker et al. [70]. The use of polarized MW irradiation combined with x-ray fluorescence technique has shown a preferential ionic migration in the polarized axis of the radiation (Figure 4a–b).

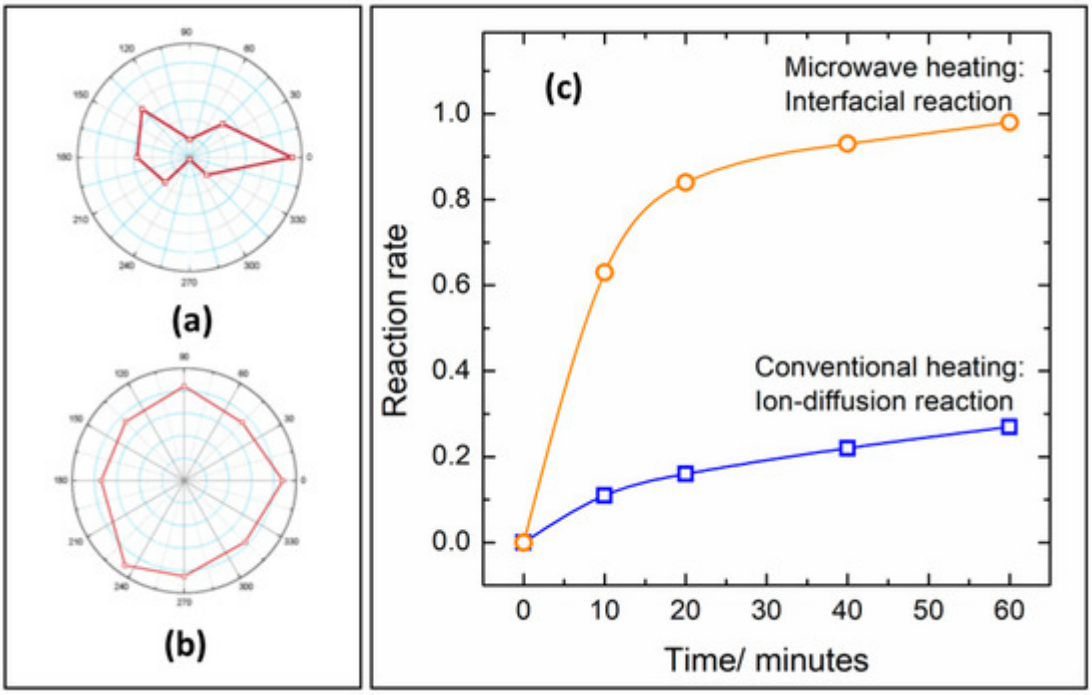

Figure 4. Ionic diffusion in a ceramic heated by polarized microwave irradiation (**a**) and conventional heating (**b**). Adapted from reference [70]. Reaction rates of $NiFe_2O_4$ synthesis under microwave heating (orange) and resistive heating (blue) at 850 °C (**c**). Adapted from ref. [71]. Copyright © 2005, American Chemical Society.

The increased diffusion is related to increased reaction rates in microwave-heated synthesis in comparison with resistive furnaces. Vanetsev et al. [71]. studied the kinetics of $NiFe_2O_4$ formation by conventional and microwave-assisted solid-state reaction. Besides the faster reaction rates, microwave irradiation also promotes changes in the rate-controlling stage of the synthesis. By removing the diffusion hindrances due to non-thermal ponderomotive forces, the rate-controlling step of the synthesis changes from ion-diffusion to the interfacial chemical reaction step (Figure 4c) [71].

Instantaneous heating is also an essential feature of dielectric heating, swiftly converting the MW energy into heat. Correspondingly, once the microwave irradiation is ceased, the heating stops immediately, causing the reaction to quench instantaneously. This could lead to metastable phases, otherwise impossible to synthesize using conventional methods. The temperature quenching can be greatly beneficial for persistent luminescence phosphors because of the defect structure caused by rapid heating and cooling rates.

Once the dielectric constant and tangent loss vary with the material composition and structure, microwave irradiation allows for selective heating of the reactants [64]. This effect can find incredible applications on heating specific sites in supported metal catalysts [72]. The synthesis of chalcogenides greatly benefits the selective heating, allowing the reaction to occur before the sulfur evaporation [73].

The properties of microwave-assisted heating are summarized in Figure 5. The combination of features allows for the synthesis of highly efficient luminescent materials with singular properties, as will be discussed in detail in the

next sections.

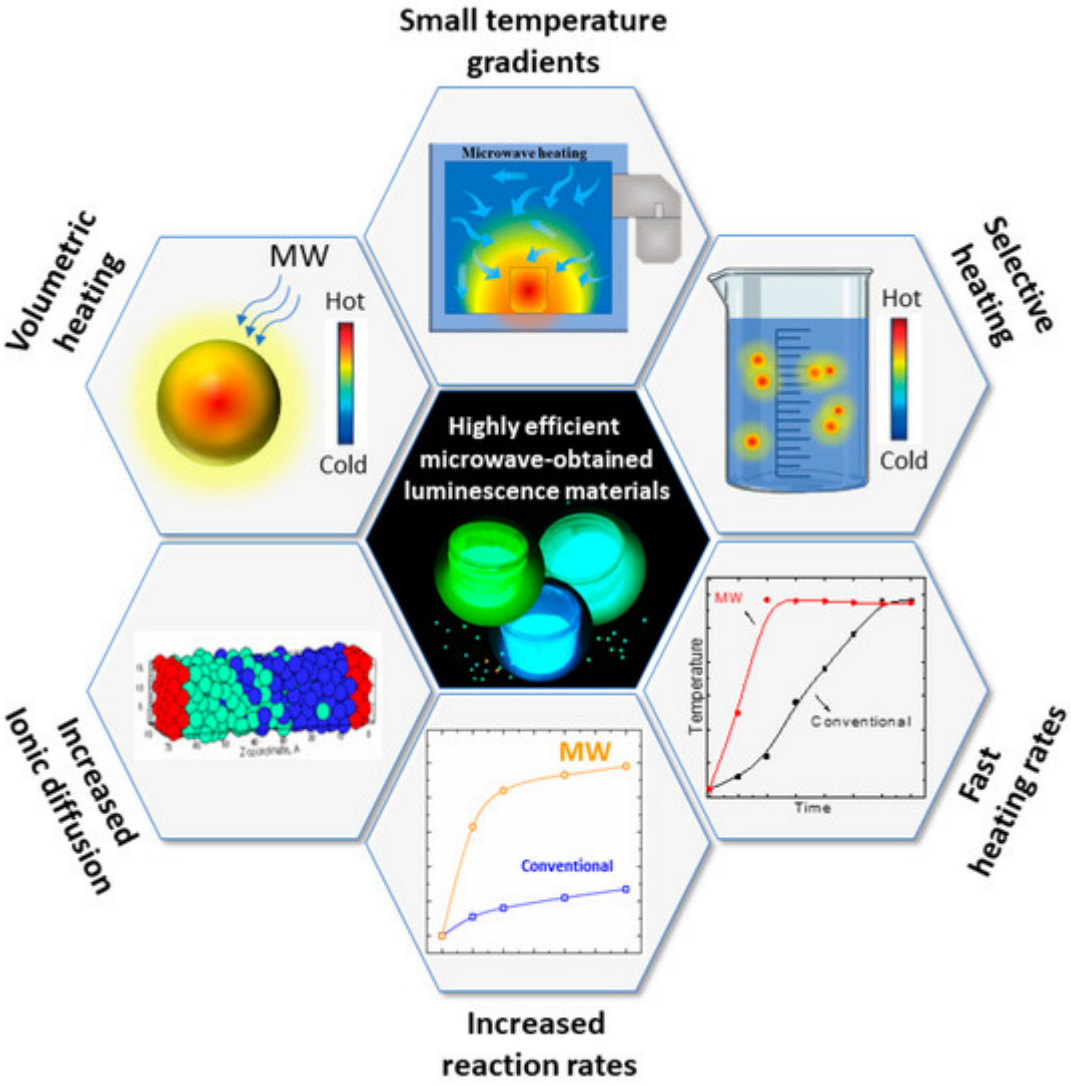

Figure 5. Fundamental microwave-assisted heating properties that are beneficial in preparing luminescent materials.

References

1. Blasse, G.; Grabmaier, B.C. Luminescent Materials; Springer: Berlin/Heidelberg, Germany, 1994; ISBN 978-3-540-58019-5.
2. Ronda, C. Rare-Earth Phosphors: Fundamentals and Applications. In Reference Module in Materials Science and Materials Engineering; Elsevier: Amsterdam, The Netherlands, 2017; ISBN 9780128035818.
3. Malta, O.L.; Brito, H.F.; Menezes, J.F.S.; e Silva, F.R.G.; Alves, S.; Farias, F.S.; de Andrade, A.V.M. Spectroscopic properties of a new light-converting device Eu(thenoyltrifluoroacetonate)3

2(dibenzyl sulfoxide). A theoretical analysis based on structural data obtained from a sparkle model. J. Lumin. 1997, 75, 255–268.

4. Rodrigues, L.C.V. Preparação e desenvolvimento do mecanismo da luminescência persistente de materiais dopados com íons terras raras. Doctoral Thesis, University of São Paulo, Butanta, Brazil, 2012.
5. Verstraete, R.; Sijbom, H.F.; Joos, J.J.; Korthout, K.; Poelman, D.; Detavernier, C.; Smet, P.F. Red Mn4+-Doped Fluoride Phosphors: Why Purity Matters. ACS Appl. Mater. Interfaces 2018, 10, 18845–18856.
6. da Silva, M.N.; Carvalho, J.M.; de Abreu Fantini, M.C.; Chiavacci, L.A.; Bourgaux, C. Nanosized ZnGa2O4:Cr3+ Spinels as Highly Luminescent Materials for Bioimaging. ACS Appl. Nano Mater. 2019, 2, 6918–6927.
7. Ming, H.; Liu, S.; Liu, L.; Peng, J.; Fu, J.; Du, F.; Ye, X. Highly Regular, Uniform K3ScF6:Mn4+ Phosphors: Facile Synthesis, Microstructures, Photoluminescence Properties, and Application in Light-Emitting Diode Devices. ACS Appl. Mater. Interfaces 2018, 10, 19783–19795.
8. Aarts, L.; van der Ende, B.; Reid, M.F.; Meijerink, A. Downconversion for solar cells in YF3:Pr3+,Yb3+. Spectrosc. Lett. 2010, 43, 373–381.
9. Terra, I.A.A.; Borrero-González, L.J.; Carvalho, J.M.; Terrile, M.C.; Felinto, M.C.F.C.; Brito, H.F.; Nunes, L.A.O. Spectroscopic properties and quantum cutting in Tb3+–Yb3+ co-doped ZrO2 nanocrystals. J. Appl. Phys. 2013, 113, 073105.
10. Vergeer, P.; Vlugt, T.J.H.; Kox, M.H.F.; Den Hertog, M.I.; Van Der Herden, J.P.J.M.; Meijerink, A. Quantum cutting by cooperative energy transfer in YbxY1-xPO4:Tb3+. Phys. Rev. B Condens. Matter Mater. Phys. 2005, 71, 1–11.
11. Yi, G.S.; Chow, G.M. Synthesis of hexagonal-phase NaYF4:Yb,Er and NaYF4:Yb,Tm nanocrystals with efficient up-conversion fluorescence. Adv. Funct. Mater. 2006, 16, 2324–2329.
12. Hu, L.; Wang, P.; Zhao, M.; Liu, L.; Zhou, L.; Li, B.; Albaqami, F.H.; El-Toni, A.M.; Li, X.; Xie, Y.; et al. Near-infrared rechargeable “optical battery” implant for irradiation-free photodynamic therapy. Biomaterials 2018, 163, 154–162.
13. Auzel, F. Upconversion and Anti-Stokes Processes with f and d Ions in Solids. Chem. Rev. 2004, 104, 139–173.
14. Smits, K.; Grigorjeva, L.; Millers, D.; Sarakovskis, A.; Opalinska, A.; Fidelus, J.D.; Lojkowski, W. Europium doped zirconia luminescence. Opt. Mater. 2010, 32, 827–831.
15. Yang, C.; Fu, L.M.; Wang, Y.; Zhang, J.P.; Wong, W.T.; Ai, X.C.; Qiao, Y.F.; Zou, B.S.; Gui, L.L. A highly luminescent europium complex showing visible-light-sensitized red emission: Direct observation of the singlet pathway. Angew. Chemie. Int. Ed. 2004, 43, 5010–5013.

16. Pappalardo, R. Calculated quantum yields for photon-cascade emission (PCE) for Pr3+ and Tm3+ in fluoride hosts. J. Lumin. 1976, 14, 159–193.
17. Piper, W.W.; DeLuca, J.A.; Ham, F.S. Cascade fluorescent decay in Pr3+-doped fluorides: Achievement of a quantum yield greater than unity for emission of visible light. J. Lumin. 1974, 8, 344–348.
18. Wegh, R.T.; Donker, H.; Oskam, K.D.; Meijerink, A. Visible quantum cutting in LiGdF4:Eu3+ through downconversion. Science 1999, 283, 663–666.
19. Wegh, R.; Donker, H.; van Loef, E.V.; Oskam, K.; Meijerink, A. Quantum cutting through downconversion in rare-earth compounds. J. Lumin. 2000, 87–89, 1017–1019.
20. Sommerdijk, J.L.; Bril, A.; de Jager, A.W. Two photon luminescence with ultraviolet excitation of trivalent praseodymium. J. Lumin. 1974, 8, 341–343.
21. Bloembergen, N. Solid State Infrared Quantum Counters. Phys. Rev. Lett. 1959, 2, 84–85.
22. Zhou, B.; Shi, B.; Jin, D.; Liu, X. Controlling upconversion nanocrystals for emerging applications. Nat. Nanotechnol. 2015, 10, 924–936.
23. Xu, J.; Tanabe, S. Persistent luminescence instead of phosphorescence: History, mechanism, and perspective. J. Lumin. 2019, 205, 581–620.
24. Van den Eeckhout, K.; Poelman, D.; Smet, P.F. Persistent luminescence in Non-Eu2+-Doped compounds: A review. Materials 2013, 6, 2789.
25. Van den Eeckhout, K.; Smet, P.F.; Poelman, D. Persistent Luminescence in Eu2+-Doped Compounds: A Review. Materials 2010, 3, 2536–2566.
26. Im, W.B.; George, N.; Kurzman, J.; Brinkley, S.; Mikhailovsky, A.; Hu, J.; Chmelka, B.F.; Denbaars, S.P.; Seshadri, R. Efficient and color-tunable oxyfluoride solid solution phosphors for solid-state white lighting. Adv. Mater. 2011, 23, 2300–2305.
27. Im, W.B.; Brinkley, S.; Hu, J.; Mikhailovsky, A.; Denbaars, S.P.; Seshadri, R. Sr2.975-xBaxCe0.025AlO4F: A highly efficient green-emitting oxyfluoride phosphor for solid state white lighting. Chem. Mater. 2010, 22, 2842–2849.
28. Dorenbos, P. Ce3+ 5d-centroid shift and vacuum referred 4f-electron binding energies of all lanthanide impurities in 150 different compounds. J. Lumin. 2013, 135, 93–104.
29. Yamaga, M.; Yosida, T.; Hara, S.; Kodama, N.; Henderson, B. Optical and electron spin resonance spectroscopy of Ti3+ and Ti4+ in Al2O3. J. Appl. Phys. 1994, 75, 1111–1117.
30. Katumo, N.; Gao, G.; Laufer, F.; Richards, B.S.; Howard, I.A. Smartphone-Based Luminescent Thermometry via Temperature-Sensitive Delayed Fluorescence from Gd2 O2 S:Eu3+. Adv. Opt. Mater. 2020, 8, 2000507.

31. Chen, R.; Pagonis, V. Modelling thermal activation characteristics of the sensitization of thermoluminescence in quartz. J. Phys. D Appl. Phys. 2004, 37, 159–164.
32. Chen, R.; Pagonis, V.; Lawless, J.L. Evaluated thermoluminescence trapping parameters-What do they really mean? Radiat. Meas. 2016, 91, 21–27.
33. Kristianpoller, N.; Chen, R.; Israeli, M. Dose dependence of thermoluminescence peaks. J. Phys. D Appl. Phys. 1974, 7, 1063–1072.
34. Dong, H.; Du, S.R.; Zheng, X.Y.; Lyu, G.M.; Sun, L.D.; Li, L.D.; Zhang, P.Z.; Zhang, C.; Yan, C.H. Lanthanide Nanoparticles: From Design toward Bioimaging and Therapy. Chem. Rev. 2015, 115, 10725–10815.
35. Wang, Q.; Liu, N.; Hou, Z.; Shi, J.; Su, X.; Sun, X. Radioiodinated Persistent Luminescence Nanoplatform for Radiation-Induced Photodynamic Therapy and Radiotherapy. Adv. Healthc. Mater. 2021, 10, 2000802.
36. Liu, J.; Lécuyer, T.; Seguin, J.; Mignet, N.; Scherman, D.; Viana, B.; Richard, C. Imaging and therapeutic applications of persistent luminescence nanomaterials. Adv. Drug Deliv. Rev. 2019, 138, 193–210.
37. Tan, H.; Wang, T.; Shao, Y.; Yu, C.; Hu, L. Crucial Breakthrough of Functional Persistent Luminescence Materials for Biomedical and Information Technological Applications. Front. Chem. 2019, 7.
38. Smet, P.F.; Parmentier, A.B.; Poelman, D. Selecting Conversion Phosphors for White Light-Emitting Diodes. J. Electrochem. Soc. 2011, 158, R37.
39. Schubert, E.F.; Kim, J.K. Solid-state light sources getting smart. Science 2005, 308, 1274–1278.
40. George, N.C.; Denault, K.A.; Seshadri, R. Phosphors for Solid-State White Lighting. Annu. Rev. Mater. Res. 2013, 43, 481–501.
41. Sijbom, H.F.; Verstraete, R.; Joos, J.J.; Poelman, D.; Smet, P.F. K2SiF6:Mn4+ as a red phosphor for displays and warm-white LEDs: A review of properties and perspectives. Opt. Mater. Express 2017, 7, 3332.
42. Saradhi, M.P.; Boudin, S.; Varadaraju, U.V.; Raveau, B. A new BaB2Si2O8:Eu2/Eu3, Tb3phosphor Synthesis and photoluminescence properties. J. Solid State Chem. 2010, 183, 2496–2500.
43. Hızal Abacı, Ö.C.; Mete, E.; Esenturk, O.; Yılmaz, A. Tunable optical properties and DFT calculations of RE3+ codoped LaBO3 phosphors. Opt. Mater. 2019, 98, 3–12.
44. Andrade, A.B.; Bispo, G.F.C.; Macedo, Z.S.; Valerio, M.E.G. Synthesis and characterization of luminescent Ln3+ (Ln = Eu, Tb and Dy)-doped LiYF4 microcrystals produced by a facile microwave-assisted hydrothermal method. J. Lumin. 2020, 219, 116843.

45. Chuang, Y.J.; Zhen, Z.; Zhang, F.; Liu, F.; Mishra, J.P.; Tang, W.; Chen, H.; Huang, X.; Wang, L.; Chen, X.; et al. Photostimulable near-infrared persistent luminescent nanoprobes for ultrasensitive and longitudinal deep-tissue bio-imaging. Theranostics 2014, 4, 1112–1122.
46. Kang, F.; Sun, G.; Boutinaud, P.; Wu, H.; Ma, F.-X.; Lu, J.; Gan, J.; Bian, H.; Gao, F.; Xiao, S. Recent advances and prospects of persistent luminescent materials as inner secondary self-luminous light source for photocatalytic applications. Chem. Eng. J. 2021, 403, 126099.
47. Van der Heggen, D.; Joos, J.J.; Rodríguez Burbano, D.C.; Capobianco, J.A.; Smet, P.F. Counting the photons: Determining the absolute storage capacity of persistent phosphors. Materials 2017, 10, 867.
48. Van der Heggen, D.; Joos, J.; Smet, P.F. On the importance of evaluating the intensity dependency of the quantum efficiency: Impact on LEDs and persistent phosphors. ACS Photonics 2018, 5, 4529–4537.
49. Bhattacharya, M.; Basak, T. A review on the susceptor assisted microwave processing of materials. Energy 2016, 97, 306–338.
50. Schiffmann, R.F. Microwave and dielectric drying. In Handbook of Industrial Drying, 4th ed.; CRC Press: Boca Raton, FL, USA, 2014; ISBN 9781466596665.
51. Kitchen, H.J.; Vallance, S.R.; Kennedy, J.L.; Tapia-Ruiz, N.; Carassiti, L.; Harrison, A.; Whittaker, A.G.; Drysdale, T.D.; Kingman, S.W.; Gregory, D.H. Modern microwave methods in solid-state inorganic materials chemistry: From fundamentals to manufacturing. Chem. Rev. 2014, 114, 1170–1206.
52. Rao, K.J.; Ramesh, P.D. Use of microwaves for the synthesis and processing of materials. Bull. Mater. Sci. 1995, 18, 447–465.
53. Naitoh, K.; Takizawa, T.; Matsuse, T. Controlled microwave irradiation for the synthesis of YBa2Cu3O7-x superconductors. Jpn. J. Appl. Phys. Part 2 Lett. 1999.
54. Vaidhyanathan, B.; Balaji, K.; Rao, K.J. Microwave-Assisted Solid-State Synthesis of Oxide Ion Conducting Stabilized Bismuth Vanadate Phases. Chem. Mater. 1998, 10, 3400–3404.
55. Rao, K.J.; Vaidhyanathan, B.; Ganguli, M.; Ramakrishnan, P.A. Synthesis of inorganic solids using microwaves. Chem. Mater. 1999, 11, 882–895.
56. Kappe, C.O. Controlled microwave heating in modern organic synthesis. Angew. Chem. Int. Ed. 2004, 43, 6250–6284.
57. Miranda De Carvalho, J.; Van Der Heggen, D.; Martin, L.I.D.J.; Smet, P.F. Microwave-assisted synthesis followed by a reduction step: Making persistent phosphors with a large storage capacity. Dalt. Trans. 2020, 49, 4518–4527.

58. Sebastian, M.T. Dielectric Materials for Wireless Communication; Elsevier: Amsterdam, The Netherlands, 2008; ISBN 9780080453309.
59. Hotta, M.; Hayashi, M.; Lanagan, M.T.; Agrawal, D.K.; Nagata, K. Complex permittivity of graphite, carbon black and coal powders in the ranges of X-band frequencies (8.2 to 12.4 ghz) and between 1 and 10 ghz. ISIJ Int. 2011, 51, 1766–1772.
60. Balanis, C.A. (Ed.) Advanced Engineering Electromagnetics; Wiley: Hoboken, NJ, USA, 2007; ISBN 9780470589489.
61. Gupta, M.; Eugene, W.W.L. Microwaves and Metals; John Wiley & Sons: Hoboken, NJ, USA, 2011; ISBN 9780470822722.
62. Pedroso, C.C.S.; Carvalho, J.M.; Rodrigues, L.C.V.; Hölsä, J.; Brito, H.F. Rapid and Energy-Saving Microwave-Assisted Solid-State Synthesis of Pr3+-, Eu3+-, or Tb3+-Doped Lu2O3Persistent Luminescence Materials. ACS Appl. Mater. Interfaces 2016, 8, 19593–19604.
63. Levin, E.E.; Grebenkemper, J.H.; Pollock, T.M.; Seshadri, R. Protocols for High Temperature Assisted-Microwave Preparation of Inorganic Compounds. Chem. Mater. 2019, 31, 7151–7159.
64. Bykov, Y.V.; Rybakov, K.I.; Semenov, V.E. High-temperature microwave processing of materials. J. Phys. D Appl. Phys. 2001, 34, R55–R75.
65. Ku, H.S.; Ball, J.A.R.; Siores, E. Review-Microwave Processing of Materials: Part III. HKIE Trans. 2001, 8, 44–50.
66. Metaxas, A.C.; Meredith, R.J. Dielectric loss. In Industrial Microwave Heating; IET: Six Hills Way, UK, 2011; pp. 5–25.
67. Li, W.; Adlung, M.; Zhang, Q.; Wickleder, C.; Schmedt auf der Günne, J. A Guide to Brighter Phosphors-Linking Luminescence Properties to Doping Homogeneity Probed by NMR. ChemPhysChem 2019, 20, 3245–3250.
68. Clark, D.E.; Folz, D.C.; West, J.K. Processing materials with microwave energy. Mater. Sci. Eng. A 2000, 287, 153–158.
69. Gusarov, V.V. Fast Solid-Phase Chemical Reactions. Russ. J. Gen. Chem. 1997, 67, 1846–1851.
70. Whittaker, A.G. Diffusion in microwave-heated ceramics. Chem. Mater. 2005, 17, 3426–3432.
71. Vanetsev, A.S.; Baranchikov, A.E.; Tret'yakov, Y.D. Kinetics of microwave-enhanced solid-phase reaction of NiFe2O4 formation. Russ. J. Inorg. Chem. 2008, 53, 495–498.
72. Rödiger, K.; Dreyer, K.; Gerdes, T.; Willert-Porada, M. Microwave sintering of hardmetals. Int. J. Refract. Met. Hard Mater. 1998, 16, 409–416.
73. dos Santos, D.O.A.; Giordano, L.; Barbará, M.A.S.G.; Portes, M.C.; Pedroso, C.C.S.; Teixeira, V.C.; Lastusaari, M.; Rodrigues, L.C.V. Abnormal co-doping effect on the red persistent

luminescence SrS:Eu2+,RE3+ materials. Dalt. Trans. 2020, 49, 16386–16393.